Supporting Information for

Amyloid-templated polydopamine nanofibers for catecholic immobilization of catalytic noble metal nanoparticles

Lv Lili,[†a] Wang Yanwei,[†b] You jun,[*c] Li mingjie,[*b] and Li Chaoxu[*b]

[a]Instrumental Analysis Center of Qingdao University, Qingdao University. Ningxia Road 308, Qingdao 266071, P.R. China.

[b]Group of Biomimetic Smart Materials, Qingdao Institute of Bioenergy and Bioprocess Technology, Chinese Academy of Sciences & Shandong Energy Institute, Songling Road 189, Qingdao 266101, P.R. China.

[c]School of Materials Science and Engineering, Hubei University, Wuhan, 30062, P.R. China

Corresponding Authors: E-mail: yjgreen123@hubu.edu.cn, limj@qibebt.ac.cn; licx@qibebt.c.cn.

Experimental Section

Materials

Dopamine (hydrochloride, purity 98%) and lysozyme were purchased from Sigma Aldrich. $AgNO_3$ and H_2PtCl_6 were brought from Solarbio science & technology Co., Ltd. $HAuCl_4$ (48% Au basis) was purchased from Sigma-Aldrich. 4-nitrophenol, NaOH, HCl and other reagents were supplied by Sinopharm chemical reagent Co. Ltd. All of the solutions were prepared by ultrapure water (resistivity: 18.2 MΩ·cm).

Fabrication of lysozyme amyloid nanofibrils. Lysozyme was dissolved in deionized water with the concentration of 2.0 wt%, and adjusted to pH 2 by 1 M of HCl. Then the lysozyme solution was gently stirred under 60 °C for 96 h to obtain the lysozyme amyloid nanofibrils.

Fabrication of PDA nanofibers templated by amyloid nanofibrils. The as-prepared lysozyme amyloid nanofibrils were diluted to 0.2 wt% and the dispersion were adjusted to pH 8.5 by 1 M of NaOH. Then equivoluminally mixed with dopamine solution (0.05−2 mg mL^{-1} with a dopamine/amyloid mass ratio, $\Phi_{dopa/lyso}$, ranging from 0.025 to 1). The mixture was stirred at 25 °C for 24 h to obtain the polydopamine composite nanofibers, and then washed with pure water for 3 times with filtration.

PDA nanofibers as scaffold for noble metal (Ag, Au, Pt) nanoparticles. The pH of PDA nanofibers suspension (0.25 wt%) was adjusted to pH 8.5 by 1 M of NaOH or ammonium hydroxide. Then the suspension of PDA nanofibers was mixed with equivoluminal solution of $AgNO_3$ (25 mM) at 80 °C for 24 h. The reactions with

$HAuCl_4$ (25 mM) or H_2PtCl_6 (25 mM) were conducted at 60 °C for 24 h.

Catalytic activity evaluation of Ag-decorated PDA nanofibers. The reduction of 4-nitrophenol was used as a model reaction to test the catalytic activity of Ag-decorated PDA nanofibers. Typically, 4-nitrophenol (100 μL, 20 mM) and $NaBH_4$ (330 μL, 3 M) were mixed in a standard quartz cuvette (Volume: 3 mL; Path length: 1 cm). The Ag-decorated PDA nanofibers were added to catalyze the reaction with a final concentration from 5.0 to 26.2 ppm (calculated by Ag). The ultraviolet visible (UV-vis) spectrophotometer (DU800) was used to monitor the absorbance variation at 200−600 nm.

Characterization

The microstructures of the samples were characterized by scanning electron microscopy (SEM, Hitachi S-4800 instrument, Japan, operated at 10 kV) and transmission electron microscopy (TEM, Hitachi H-7650, Japan, operated at 100 kV). For SEM observation, the aqueous suspensions were dropped onto the aluminum foil, air-dried under room temperature, and sputtered with platinum before the test. For TEM measurement, the suspensions were drop-casted onto a copper grid with carbon film. Contrast of nanofibrils was achieved by negative staining through adding a droplet of 1 wt% uranyl acetate solution (Sigma-Aldrich) onto the grid and allowing the staining to occur over a period of 2 h; any excess of staining agent was removed by a filter paper. X-ray diffraction (XRD) measurements were taken on an X-ray diffractometer (Bruker D8 ADVANCE) using Cu Kα (λ = 1.5406 Å) radiation. The average crystallite size of Ag NPs was calculated by the XRD pattern parameters

according to the Scherrer equation: $D = \frac{K\lambda}{\beta Cos\,\theta}$, where D is the size of Ag NPs, K is 0.89, λ is the X-ray wavelength of Cu Kα (λ = 1.5406 Å), β (in radians) is the full-width at half-maximum of the observed peak, and θ is the Bragg's diffraction angle of the observed peak. Thermal gravimetric analysis (TGA) was performed on a thermogravimetric analyzer (Ulvac TGD 9600) under dry nitrogen purge at a flow rate of 10 mL min^{-1} and heated from 25 to 800 °C at the ramp rate of 10 °C min^{-1}. Fourier transforming infrared spectrum (FT-IR) was recorded on a Nicolet 6700 FT-IR spectrometer (American) using the KBr pellets method with 64 scans. X-ray photoelectron spectra (XPS) were obtained with an ESCALAB 250Xi (Thermo Scientific) X-ray photoelectron spectrometer, using monochromatic Al Kα (1486.6 eV) radiation as the excitation source.

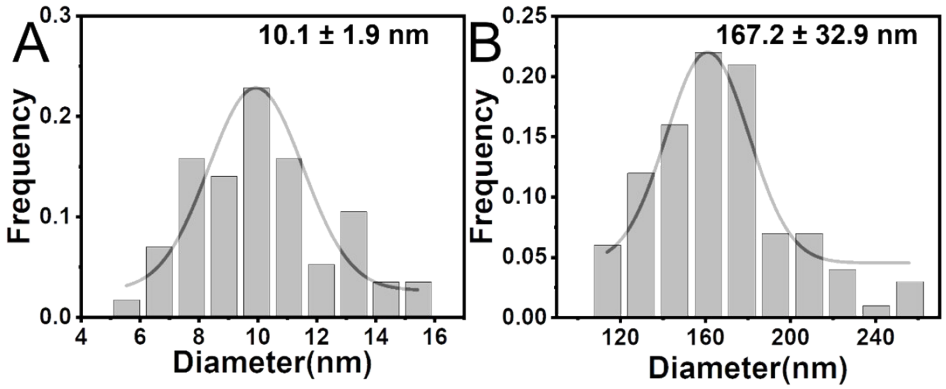

Fig. S1. (A) Diameter histogram of lysozyme amyloid nanofibrils, which averaged at 10.1 nm with standard deviation (SD) of ±1.9 nm. (B) Diameter histogram of PDA nanoparticles produced without the templates of amyloid nanofibrils. The diameters of PDA nanoparticles distributed in 110–260 nm, averaged at 167.2 nm with SD of ±32.9 nm.

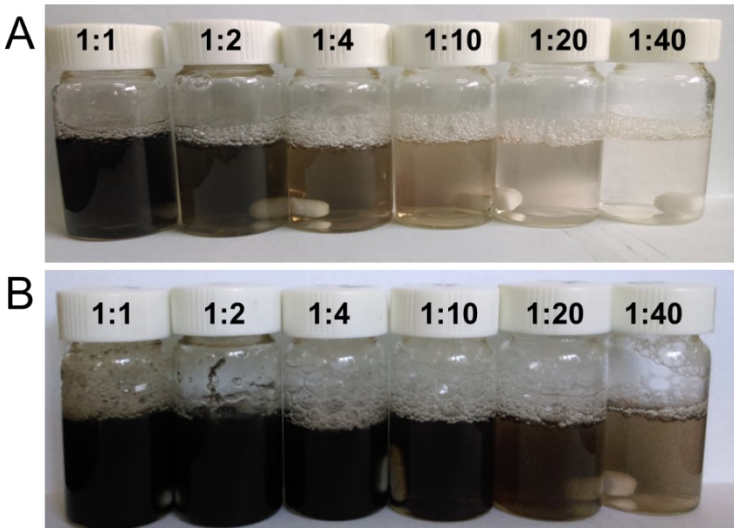

Fig. S2. (A) Optical images of dispersion of dopamine and lysozyme nanofibrils with different weight ratios (dopamine/amyloid mass ratio, $\Phi_{dopa/lyso}$). (B) Optical images of dispersion of PDA composite nanofibers on the templates of lysozyme nanofibrils after reaction at pH 8.5 and 25 °C for 12 h.

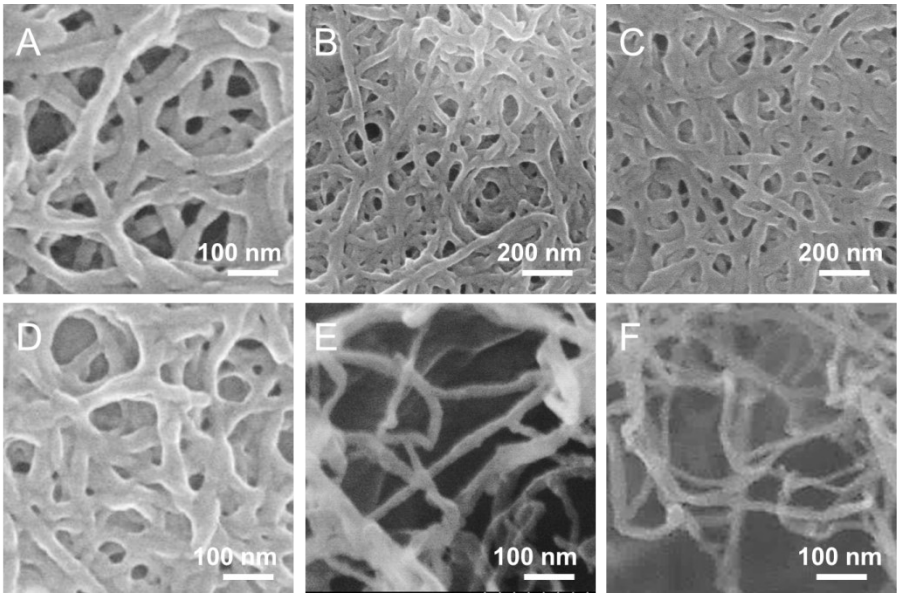

Fig. S3. SEM images of PDA composite nanofibers on the templates of lysozyme nanofibrils with different initial dopamine to lysozyme nanofibrils weight ratios: (A) 1, (B) 0.5, (C) 0.25, (D) 0.1, (E) 0.05, and (F) 0.025.

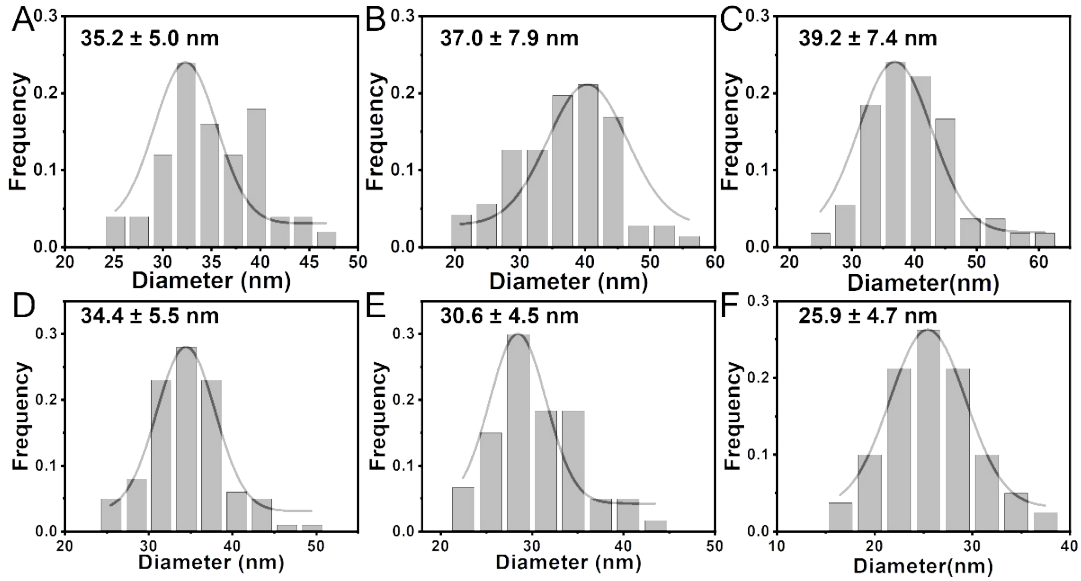

Fig. S4. Diameter histogram of PDA composite nanofibers on the templates of lysozyme nanofibrils with different initial dopamine to lysozyme nanofibrils weight ratios: (A) 1, the average diameter of 35.2 nm with SD of ±5.0 nm, (B) 0.5, the average diameter was 37.0 nm with SD of ±7.9 nm, (C) 0.25, the average diameter

was 39.2 nm with SD of ±7.4 nm, (D) 0.1, the average diameter was 34.4 nm with SD of ±5.5 nm, (E) 0.05, the average diameter was 30.6 nm with SD of ±4.5 nm, and (F) 0.025, the average diameter was 25.9 nm with SD of ±4.7 nm. With higher $\Phi_{dopa/lyso}$ (e.g., 0.5–1), the diameter seemed constant (35–37 nm) without further increase, which should be due to the formation of free PDA particles in the solution.

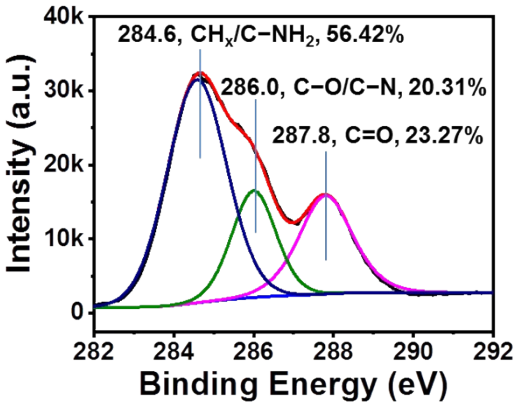

Fig. S5. High-resolution C1s XPS spectrum of PDA composite nanofibers.

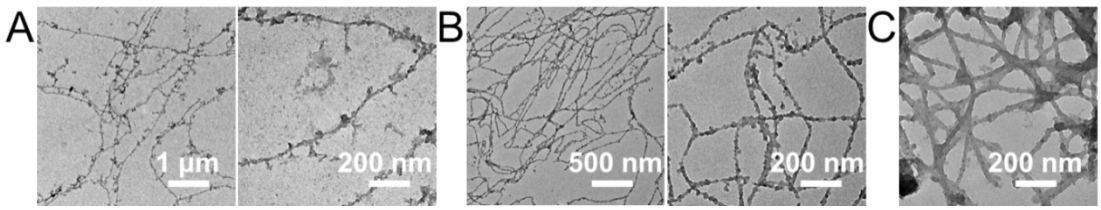

Fig. S6. TEM images of (A) rhodanine nanofibers, (B) tripolycyanamide nanofibers, and (C) tannic acid nanofibers on the templates of lysozyme amyloid nanofibrils.

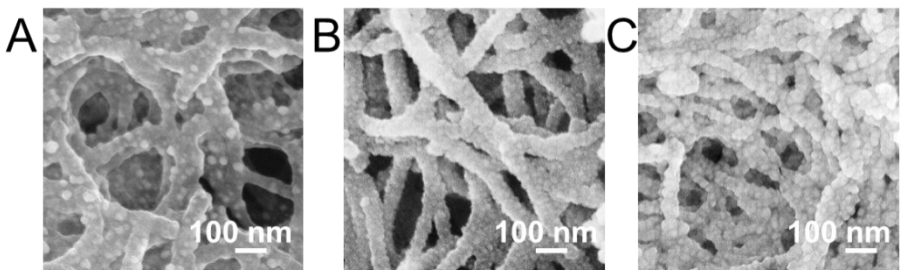

Fig. S7. SEM images of Ag NPs on the templates of PDA composite nanofibers

obtained at (A) pH 2, (B) pH 8.5, and (C) pH 10. The numbers of Ag NPs on the fiber with per unit length was evaluated. At pH 2, there were 5–7 Ag NPs per 100 nm length. At pH 8.5, there were 17–26 Ag NPs per 100 nm length. Therefore, a higher pH value should lead to a denser distribution of Ag NPs on the PDA composite nanofiber. As a zwitterion with an isoelectric point of ~4, PDA shell exhibited more negative charges and stronger metal ion binding capability at higher pH values (>4) due to deprotonation of catechol. Whereas, at pH value (e.g., 2) under isoelectric point, positive charge from amino groups of PDA shell might arouse electrostatic repulsion towards Ag^{+} and hinder the chelating ability, thus generated less Ag NPs.

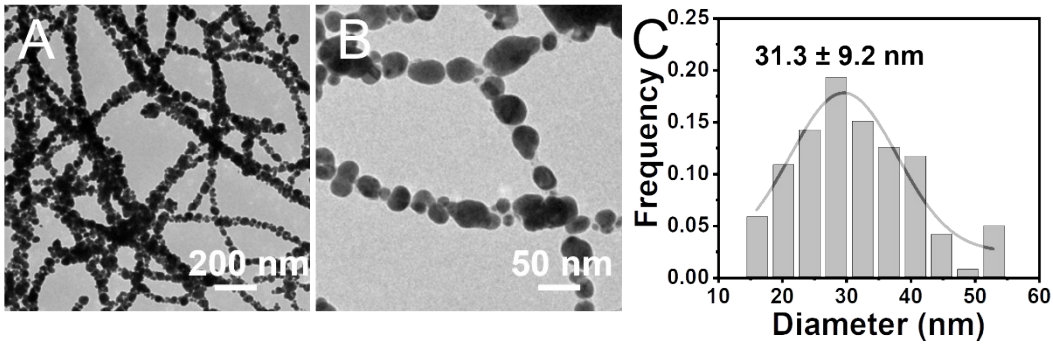

Fig. S8. (A-B) TEM images and (C) diameter histogram of Ag NPs on the templates of PDA composite nanofibers obtained at pH 10. The average diameter of Ag NPs obtained at pH 10 was 31.3 nm with SD of ±9.2 nm, much larger than that of Ag NPs obtained at pH 8.5 (14.2 nm with SD of ±2.9 nm).

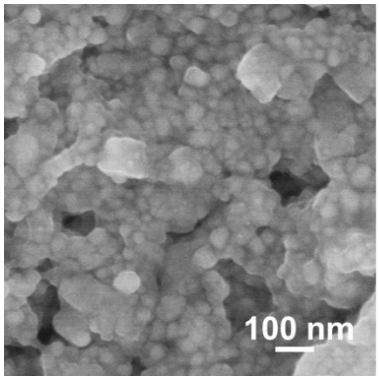

Fig. S9. SEM images of Ag NPs obtained with weight ratio of PDA composite nanofibers to Ag^{+} of 1:2.

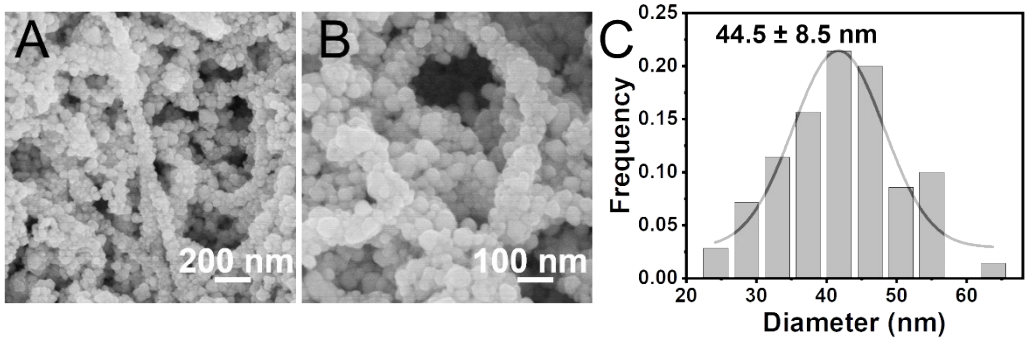

Fig. S10. (A-B) SEM images and (C) Diameter histogram of Ag NPs on PDA composite nanofibers obtained at temperature at 60 °C.

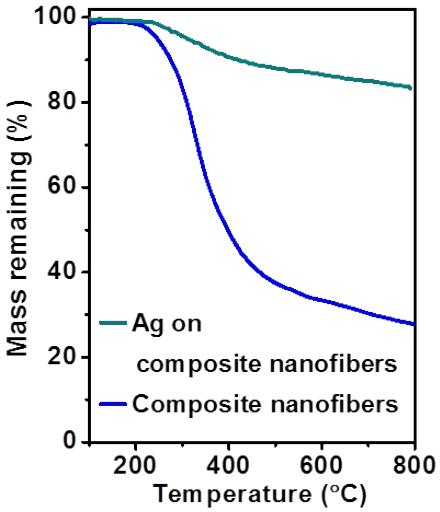

Fig. S11. Thermal gravimetric analysis (TGA) curves of Ag NPs on PDA composite nanofibers and PDA composite nanofibers.

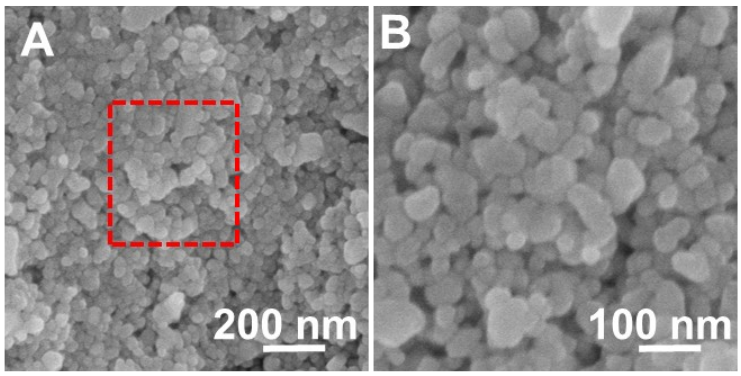

Fig. S12. SEM images of Ag NPs deposited on lysozyme nanofibrils.

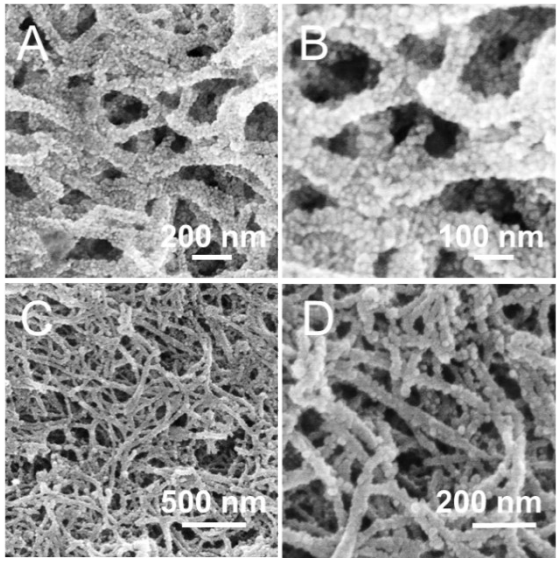

Fig. S13. SEM images of (A-B) Au NPs and (C-D) Pt NPs on PDA composite nanofibers obtained at pH 8.5.

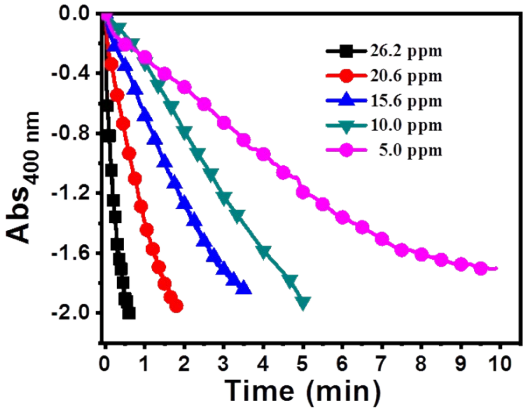

Fig. S14 Catalytic activity at different concentrations of catalysts by monitoring the absorbance at 400 nm. With the initial 4-NP concentration of 10^{-4} mol/L and $NaBH_4$ concentration of 0.1 mol/L.

Table S1. Catalytic activity comparisons of Ag NPs on PDA composite fibers with previous reported Ag NPs based catalysts.

Catalyst	Size (nm)	Rate Constant (k, min^{-1})	Reference
Ag NPs	5	0.23	S1
Cu-Ag Bimetallic Nanoparticles	40.3	0.237	S2
Ag/CeO_2	5–20	0.656	S3
Fe_3O_4/Ag@Ca-Al LDH hybrid	4.2	0.318	S4
Fe_3O_4@PS/PDA-Ag	10	0.393	S5
Ag nanocomposites	12	2.944	S6
Ag NPs on GO/Dopa	7.71	0.364	S7
Ag NPs on PANFs	10–25	0.055	S8
Ag/GO nanocomposites	50	0.493	S9
Ag NPs/HTO-PDA	53	0.184	S10
PP-g-EDA@Ag/Cu	--	0.248	S11
Ag/Nanosilica	20	0.0459	S12
Ag/C spheres	10	0.1014	S13
Ag NPs on PDA fibers	14	0.37	This Work

Notes:

LDH: layer double hydroxide.[S4] PS: Polystyrene.[S5] PDA: polydopamine.[S5] GO: graphene oxide.[S7,S9] PANFs: polyacrylonitrile fibers.[S8] HTO-PDA: hollow-tubular-oriented polydopamine.[S10] PP-g-EDA: polypropylene grafting ethylenediamine.[S11]

References:

S1 J. Min, F. Wang, Y. Cai, S. Liang, Z. Zhang and X. Jiang, *Chem. Commun.*, 2015, **51**, 761-764.

S2 W. Wu, M. Lei, S. Yang, L. Zhou, L. Liu, X. Xiao, C. Jiang and V. A. L. Roy, *J. Mater. Chem. A*, 2015, **3**, 3450-3455.

S3 M. Chernykh, N. Mikheeva, V. Zaikovskii, M. Salaev, L. E. Liotta and G. Mamontov, *Catalysts*, 2020, **10**, 580.

S4 M. Dinari and F. Dadkhah, *Carbohydr. Polym.*, 2020, **228**, 115392.

S5 F. Peng, Q. Wang, R. Shi, Z. Wang, X. You, Y. Liu, F. Wang, J. Gao and C. Mao, *Sci. Rep.*, 2016, **6**, 39502.

S6 S. S. Pi, F. Ma, D. Cui, L. Feng, L. Zhou and A. Li, *Environ. Res.*, 2021, **197**, 111006.

S7 E. K. Jeon, E. Seo, E. Lee, W. Lee, M.-K. Um and B. S. Kim, *Chem. Commun.*, 2013, **49**, 3392-3394.

S8 J. Xiao, Z. Y. Wu, K. L. Li, Z. B. Zhao and C. N. Liu, *RSC Adv.*, 2021, **12**, 1051-1061.

S9 Y. Z. Li, Y. L. Cao, J. Xie, D. Z. Jia, H. Y. Qin and Z. T. Liang, *Catal. Commun.*, 2015, **58**, 21-25.

S10 E. J. Cao, W. Z. Duan, F. Wang, A. Q. Wang and Y. Zheng, *Carbohydr. Polym.*, 2017, **158**, 44-50.

S11 X. Q. Zhang, R. F. Shen, X. J. Guo, X. Yan, Y. Chen, J. T. Hu and W. Z. Lang, *Chem. Eng. J.*, 2021, **408**, 128018.

S12 S. K. Das, M. M. R. Khan, A. K. Guha and N. Naskar, *Green Chem.*, 2013, **15**, 2548-2557.

S13 S. Tang, S. Vongehr and X. Meng, *J. Mater. Chem.*, 2010, **20**, 5436-5445.